THE JOURNAL OF BIOLOGICAL CHEMISTRY VOL. 288, NO. 17, pp. 11887–11896, April 26, 2013

Dual Functions for Cytosolic α-Mannosidase (Man2C1)

ITS DOWN-REGULATION CAUSES MITOCHONDRIA-DEPENDENT APOPTOSIS INDEPENDENTLY OF ITS α-MANNOSIDASE ACTIVITY[*S]

Received for publication, October 5, 2012, and in revised form, February 18, 2013 Published, JBC Papers in Press, March 13, 2013, DOI 10.1074/jbc.M112.425702

Li Wang and Tadashi Suzuki[1]

From the Glycometabolome Team, Systems Glycobiology Research Group, RIKEN Max Planck Joint Research Center, RIKEN Global Research Cluster, 2-1 Hirosawa, Wako, Saitama 351-0198, Japan

Background: Man2C1 regulates apoptosis via an unknown mechanism.
Results: Suppression of Man2C1 induces mitochondria-dependent apoptosis independently of its enzyme activity.
Conclusion: Man2C1 has dual functions in glycan catabolism and apoptotic signaling.
Significance: This study demonstrates that the role of Man2C1 in apoptosis is independent of its α-mannosidase activity.

Cytosolic α-mannosidase (Man2C1) trims free oligosaccharides in mammalian cells, and its down-regulation reportedly delays cancer growth by inducing mitotic arrest or apoptosis. However, the mechanism by which Man2C1 down-regulation induces apoptosis is unknown. Here, we demonstrated that silencing of Man2C1 via small hairpin RNAs induced mitochondria-dependent apoptosis in HeLa cells. Expression of CHOP (C/EBP homologous protein), a transcription factor critical to endoplasmic reticulum stress-induced apoptosis, was significantly up-regulated in *Man2C1* knockdown cells. However, this enhanced CHOP expression was not caused by endoplasmic reticulum stress. Interestingly, Man2C1 catalytic activity was not required for this regulation of apoptosis; introduction of mutant, enzymatically inactive Man2C1 rescued apoptotic phenotypes of *Man2C1* knockdown cells. These results show that Man2C1 has dual functions: one in glycan catabolism and another in apoptotic signaling.

N-Glycosylation is widely recognized as one of the most important modifications to eukaryotic proteins. Moreover, *N*-glycans on proteins have crucial roles; they can affect physicochemical properties of the proteins (*e.g.*, protein solubility or stability) and physiological properties (*e.g.*, bioactivity or intra-/intercellular trafficking) (1, 2). The biosynthetic pathways leading to *N*-glycosylation in mammalian cells are well understood, and genetically modified animal models allow us to assess the importance of specific sugar modifications in great detail (3, 4). However, the molecular details of the catabolic pathways that breakdown *N*-glycan are less well understood, especially the details of the nonlysosomal degradation pathway (5, 6).

Free oligosaccharides derived from *N*-glycans on proteins or from their lipid-linked precursors accumulate in the cytosol (5, 7–10). Currently, two glycosidases (endo-β-*N*-acetylglucosaminidase (11) and Man2C1 (12)) are known to be involved in the catabolism of free, high mannose-type oligosaccharides in the cytosol of mammalian cells. The processing of free oligosaccharides by these enzymes is postulated to be important for the subsequent transport of the oligosaccharides into lysosomes by a putative oligosaccharide transporter on the lysosomal membrane (13); this hypothesis is consistent with the observation that down-regulation or inhibition of Man2C1 leads to oligosaccharide accumulation in the cytosol (12, 14–17).

Reportedly, Man2C1 overexpression induces ER[2] stress (17) and promotes tumor growth and metastasis (18–20). These findings led us to speculate that this protein is a potential target for anti-cancer therapy. Suppression of the *Man2C1* gene was shown to induce growth delay or arrest in nasopharyngeal carcinoma cells (19) and in Hek293 cells (12). Down-regulation of Man2C1 reportedly also results in mitotic arrest and apoptosis in esophageal carcinoma cells (21). These results indicate that Man2C1 has a role in regulating apoptotic signaling for certain cells.

Here, we investigated the mechanism(s) by which Man2C1 suppression causes cell growth arrest and/or apoptosis. We found that *Man2C1* knockdown cells underwent apoptosis via a mitochondria-dependent pathway that involved CHOP (C/EBP homologous protein) up-regulation. Our results also show that Man2C1 had a role in apoptosis that was independent of its enzymatic activity; this finding provides convincing evidence that Man2C1 has dual functions: one as a catabolic enzyme for the breakdown of free, cytosolic oligosaccharides and another as a modulator of apoptotic signaling.

EXPERIMENTAL PROCEDURES

Cell Cultures—HeLa cells or HepG2 cells were cultured in DMEM (Nacalai Tesque Co.) supplemented with 10% fetal bovine serum and antibiotics (100 units/ml penicillin G, 100

* The work was supported in part by a Grant-in-Aid for Scientific Research from the Ministry of Education, Culture, Sports, Science and Technology of Japan and a research grant from Japan Foundation for Applied Enzymology (to T. S.).
[S] This article contains supplemental Fig. S1.
[1] To whom correspondence should be addressed: Glycometabolome Team, Systems Glycobiology Research Group, RIKEN Max Planck Joint Research Center, RIKEN Global Research Cluster, 2-1 Hirosawa, Wako, Saitama 351-0198, Japan. Tel.: 81-48-467-9614; Fax: 81-48-467-9626; E-mail: tsuzuki_gm@riken.jp.

[2] The abbreviations used are: ER, endoplasmic reticulum; PA, 2-aminopyridine; PI, propidium iodide; PTEN, phosphatase and tensin homolog; PARP, poly(ADP-ribose) polymerase.

ng/ml streptomycin; Nacalai Tesque Co.) in humidified air containing 5% CO_2 at 37 °C. MKN45 cells were cultured in RPMI 1640 (Nacalai Tesque Co.) with 10% fetal bovine serum and antibiotics (100 units/ml penicillin G, 100 ng/ml streptomycin; Nacalai Tesque Co.).

Lentiviral Vector-based Small Hairpin RNA—Sequences encoding two distinct shRNAs were each cloned into lentivirus vectors; each construct was introduced into cells either by viral infection or plasmid transfection. The two shRNAs were designed to target and knock down *Man2C1* expression. Lentiviral particles (2–15 μl, roughly 1 particle/cell, Mission® lentiviral transduction particles; Sigma) were added to 5×10^4 cells. To screen for stable transfectants, culture medium was replaced with fresh DMEM containing 0.5 μg/ml puromycin 48 h after infection. Medium was replaced every 3 or 4 days until resistant colonies were identified. The following two sequences were used for these experiments: shRNA No. 1, 5′-CCGGCGAGTTCACCTATGCACTGATCTCGAGATCAGTGCATAGGTGAACTCGTTTTTG-3′ and shRNA No. 2, 5′-CCGGCGGAACCCTGAGTTCATCTTTCTCGAGAAAGATGAACTCAGGGTTCCGTTTTTG-3′. The MISSION shRNA control vector (MISSION pLKO.1-puro Empty Vector Control Plasmid, SHC001; Sigma) was transfected into cells to isolate the control transfectants.

For plasmid transfection, 2 μg of a shRNA vector or a control vector (SHC001, described above, or MISSION pLKO.1-puro nonmammalian shRNA control plasmid, SHC002; Sigma) was transfected into 1×10^6 cells using the Nucleofactor transfected kit (Amaxa) according to the manufacturer's protocols. The cells were harvested 48 h after transfection for further examination. The sequences of Man2C1 shRNAs were the same as those above.

Plasmid Construction and Transfection—A full-length Man2C1 cDNA and two truncated Man2C1 cDNAs, an N-terminal and a C-terminal construct, were amplified and cloned into pENTR™/D-TOPO (Invitrogen); the primers 5′-CACCATGGCGGCTGCGCCGGCCTT-3′ and 5′-GTGTGGCGGAGGCTGAAG-3′ were used to amplify the full-length cDNA, 5′-CACCATGGCGGCTGCGCCGGCCTT-3′ and 5′-CAGGGCCATCACTTCGAT-3′ were used for the N-terminal construct, and primers 5′-CACCATGGCCCTGCCCAAACCG-3′ and 5′-GTGTGGCGGAGGCTGAAG-3′ for the C-terminal construct. DNA sequences of each construct were confirmed using BigDye ver.3.1 and an ABI DNA Sequencer. The gene in each pENTR vector was then transferred into the destination vector (pcDNA™6.2/V5-DEST; Invitrogen) via LR Clonase II reactions (Invitrogen) to generate V5-tagged full-length Man2C1, V5-tagged N-terminal Man2C1, and V5-tagged C-terminal Man2C1.

Each V5-tagged construct (1 μg)—full-length Man2C1, N-terminal Man2C1, and C-terminal Man2C1—was transfected into 1×10^6 cells using FuGENE 6 (Roche Applied Science) according to the manufacturer's protocols. The cells were harvested 48 h after transfection for further examination.

Quantitative Gene Expression Analyses via PCR—For real time PCR analysis, total RNA was isolated from cells with the Qiagen RNeasy kit; 4 μg of each RNA sample was reverse-transcribed with random hexamers using the SuperScript III RT kit (Invitrogen) according to the manufacturer's protocols. Each real time PCR was performed using a TaqMan Universal PCR Master Mix system (Roche Applied Science). Each final 20-μl real time PCR contained 10 μl of TaqMan Mix buffer, 1 μl of the probes provided by Roche Applied Science, and 9 μl of cDNA (0.2 μg). The cDNA was amplified by an initial step at 95 °C for 10 min, followed by 40 cycles at 95 °C for 5 s and at 55 °C for 20 s; an ABI PRISM 7900HT sequence detection system (Applied Biosystems) was used. The samples were analyzed in duplicate; the mean number of cycles to the threshold of fluorescence detection was calculated for each sample. The g*lyceraldehyde-3-phosphate dehydrogenase* (*GAPDH*) expression in each sample was measured to normalize the amount of cDNA in each sample. The *Man2C1* and *GAPDH* probes used for real time PCR were purchased from Roche Applied Science.

To examine *XBP1* transcripts via RT-PCR, total RNA was isolated and reverse-transcribed as described above. The following two primers were used to assess *XBP1* expression: sense primer, 5′-CCTTGTAGTTGAGAACCAGG-3′, and antisense primer, 5′-GGGGCTTGGTATATATGTGG-3′. To distinguish spliced *XBP1* from unspliced *XBP1*, PCR products were incubated with 1 μl of PstI (15 units/μl) at 37 °C for 30 min before being resolved on a 2% agarose gel (22).

FITC-Annexin V/Propidium Iodide (PI) Double Staining Analysis—Cultured cells were harvested, washed twice with ice-cold PBS, and suspended in 1× binding buffer (10 mM HEPES buffer, 0.14 M NaCl, 2.5 mM $CaCl_2$, pH 7.4) at a concentration of 1×10^6 cells/ml. Samples of 100 μl (1×10^5 cells) were each transferred into separate 5-ml FALCON tubes; 5 μl of FITC-annexin V (BD Biosciences) and 10 μl of PI (50 μg/ml) were added to each tube. Each cell suspension was mixed gently via vortex and then incubated for 15 min at room temperature (25 °C) in the dark; 400 μl of 1× binding buffer was then added to each suspension. The cells were subjected to flow cytometry analysis within 1 h.

PI Cell Cycle Analysis—Cultured cells (1×10^6) were harvested, then fixed, and permeabilized via treatment with 70% (w/v) ice-cold ethanol overnight at 4 °C; the cells were then washed with PBS and resuspended in 1 ml of 0.1% (v/v) Triton X-100/PBS containing 20 μg/ml PI and 500 units/ml boiled RNase A. After incubation for 15 min in the dark at room temperature, the cells were subjected to flow cytometry analysis.

Western Blot Analysis—Cultured cells (1×10^6) were washed twice with PBS and lysed at 4 °C in 500 μl of lysis buffer (1% Triton X-100, 150 mM NaCl, 25 mM Tris-HCl, pH 7.4, 5 mM EDTA) containing 1× complete protease inhibitor mixture (Roche Applied Science) and 1 mM Pefabloc (Roche Applied Science). An aliquot of each lysate was analyzed via SDS-PAGE. Following electrophoresis, separated proteins were transferred to Western blots and visualized using a LAS3000mini (Fujifilm Co.) and Immobilon Western Reagents (Millipore). The following antibodies were used in these experiments: nine primary antibodies (rabbit anti-caspase 3 (dilution; 1:3,000), rabbit anti-PARP (1:3,000), mouse anti-caspase 8 (1:3,000), rabbit anti-caspase 9 (1:3,000), mouse anti-CHOP (1:3,000), rabbit anti-BiP (1:3,000), rabbit anti-Akt (1:3,000), rabbit anti-P-Akt S473 (1:3,000), and rabbit anti-P-Akt T308 (1:3,000)) were purchased from Cell Signaling Technology, and two (mouse anti-cyto-

chrome *c* (1:3,000) and rabbit anti-VDAC (1:3,000)) were from Santa Cruz Biotechnology; mouse anti-V5 (1:5,000) was from Invitrogen; the mouse anti-GAPDH antibody (1:5,000) was from Millipore. Secondary antibodies (anti-rabbit IgG antibody (1:5,000) and anti-mouse IgG antibody (1:5,000, except for the case with anti-GAPDH (1:10,000))) were purchased from Cell Signaling Technology.

Fractionation of Cytosol and Mitochondria—HeLa cells (1×10^6) and *Man2C1* knockdown HeLa cells were washed twice with PBS, then harvested, and finally separated into cytosolic fractions and mitochondrial fractions using a Qproteome mitochondria isolation kit (Qiagen) according to the manufacturer's protocol.

Cytosolic α-Mannosidase Assay—The isolation of a cytosolic fraction from cell lysates was described above. For each 40-μl α-mannosidase assay reaction, 1 mM $CoCl_2$, 20 μl of 200 mM Mes/NaOH buffer, pH 6.7, 10 μl of substrate (*p*-nitrophenyl-α-D-mannoside final concentration, 1 mM; Sigma), and 10 μl of cytosolic fractions of the indicated cell type were mixed gently and incubated at 37 °C for 1 h. Each reaction was stopped by adding 900 μl of 0.2 M Na_2CO_3 (pH 11.4). Liberated *p*-nitrophenol was measured with a spectrophotometer set at 410 nm; one unit of enzyme was defined as the amount required to release 1 μmol of *p*-nitrophenol from *p*-nitrophenyl-α-D-mannoside in 1 h at 37 °C under the experimental condition. Total protein concentration in each crude enzyme preparation was determined via the bicinchoninic acid method (Pierce) according to the manufacturer's instructions; bovine serum albumin was used as the standard.

Extraction and Labeling of Free Oligosaccharides with 2-Aminopyridine (PA) Recovered from Cytosol—Individual aliquots of 1×10^8 cells were each washed twice with cold PBS; the cells were then harvested and lysed in 800 μl of lysis buffer (10 mM HEPES/NaOH buffer, pH 7.4, 5 mM DTT, 250 mM mannitol, 1 mM EDTA, pH 8.0, 1× complete protease inhibitor mixture, and 1 mM Pefabloc). Each cell lysate was homogenized and centrifuged at 1,000 × *g* for 10 min at 4 °C to remove nuclei and unbroken cells. Each supernatant was then centrifuged at 100,000 × *g* for 1 h at 4 °C; the resulting supernatants contained the cytosolic fractions. To precipitate proteins, ethanol (150% v/v) was added to the cytosolic fraction; each solution was mixed well and centrifuged at 17,000 × *g* for 20 min at 4 °C. Each supernatant, which contained the free oligosaccharides, was desalted using a PD-10 column (GE Healthcare) according to the manufacturer's instructions. Detailed methods for PA labeling and for removal of excess reagent were described before (23); each sample thus prepared was used for subsequent size fractionation HPLC analysis.

Size Fractionation HPLC Analysis—For size fractionation HPLC, we used a Shodex NH2P-50 4E column, in conjunction with a GL Sciences HPLC system (PU611 double pumps/CO630 column oven) with a fluorescence detector (LaChrom; Hitachi High-Technologies Co.). Elution was performed using two solvent gradients: solvent A, 93% acetonitrile in 0.3% acetate (pH adjusted to 7.0 with ammonia); and solvent B, 20% acetonitrile in 0.3% acetate (pH adjusted to 7.0 with ammonia). The gradient program, where percentage refers to the percentage of solvent A, was 0–5 min, isocratic 97%; 5–8 min, 97–67%; and 8–40 min, 67–29%. Eluted compounds were detected by fluorescence at λ_{ex} = 310 nm and λ_{em} = 380 nm. α-Mannosidase digestion of PA-labeled free oligosaccharides was carried out as described previously (23), and the α-mannosidase-sensitive peaks in the $Hex_{5-9}HexNAc$ fractions (12) were then measured. For quantification, the PA-Glc_6 in the PA-glucose oligomer (TaKaRa Bio Inc.; 2 pmol/μl) was used as a reference.

RESULTS

Down-regulation of Man2C1 by shRNA Induces HeLa Cell Apoptosis—To investigate the function of Man2C1 in growth arrest and/or cellular apoptosis, we used shRNA to down-regulate Man2C1 expression in HeLa cells. We achieved Man2C1 knockdown (49 or 51%) using two distinct shRNA vectors specific for Man2C1 (Fig. 1*A*); Man2C1 knockdown caused suppression of α-mannosidase activity (~70 or 65%, respectively) in the cytosol (Fig. 1*B*). These Man2C1 knockdown cells exhibited increased accumulation of free oligosaccharides in the cytosol (Table 1), indicating that, as with previous observations (12, 14–17), processing of cytosolic free oligosaccharides was impaired by Man2C1 down-regulation. In these Man2C1 knockdown cells, apoptosis was evident, as shown by FITC-annexin V/PI double staining. Higher numbers of annexin V^+/PI^- cells were observed in both groups of Man2C1 knockdown cells, indicating up-regulation of apoptotic signal, when compared with control cells (Fig. 1*C*). Moreover, PI cell cycle analysis revealed accumulation of cells in sub-G_1 phase (Fig. 1*D*), also indicating that the number of apoptotic cells was higher among the Man2C1 knockdown cells. Apoptotic bodies were frequently apparent in the nuclei of Man2C1 knockdown cells (supplemental Fig. S1).

Although apoptotic cells were common in stable transfectants expressing either Man2C1 shRNA, we were concerned that we had selected clones with special characteristics. This consideration was of particular concern if Man2C1 down-regulation was critical for normal cell growth and survival. We therefore tested the effect of transient transfection of Man2C1 shRNA into HeLa cells. Transient expression of either Man2C1 shRNA suppressed the Man2C1 mRNA level (56 or 58% of control) in HeLa cells (Fig. 2*A*). We also observed higher numbers of annexin V^+/PI^- cells in transiently transfected Man2C1 knockdown cells (Fig. 2*B*). These results confirm that more HeLa cells underwent apoptosis when Man2C1 was suppressed than when it was not.

Down-regulation of Man2C1 Induces Mitochondria-dependent Apoptosis—To Down-regulation of Man2C1 induces mitochondria-dependent apoptosis. To identify which apoptotic signaling pathway(s) were regulated by Man2C1, caspase 3 cleavage was examined because it is central to all caspase-dependent apoptotic signal (see Fig. 9 for a schematic view of the intrinsic and extrinsic apoptotic signaling pathways). Levels of pro-caspase 3, the inactive form of caspase 3, evidently decreased in Man2C1 knockdown cells, indicating enhanced activation of this protein (Fig. 3*A*, compare *lanes 3* and *4* with *lanes 1* and *2*). We could not detect the active (cleaved) form of caspase 3 even in the presence of MG-132, a positive inducer of cell apoptosis (24–26); therefore, we examined the processing of poly(ADP-ribose) polymerase (PARP), a major substrate of

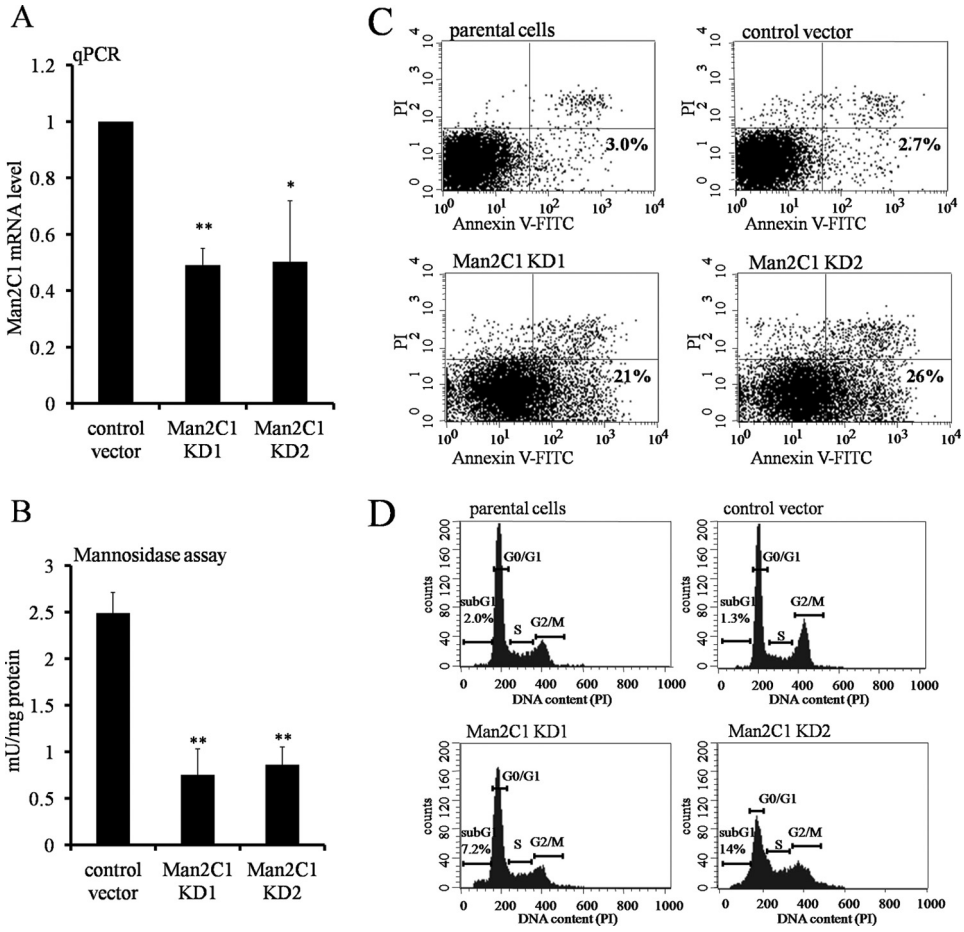

FIGURE 1. **Down-regulation of Man2C1 in HeLa cells induced apoptosis.** *A*, level of *Man2C1* expression in *Man2C1* knockdown cells. HeLa cells were infected with one of two different lentivirus-based Man2C1 shRNA vectors or a control empty vector. Stable transfectants were isolated and designated as Man2C1 KD1, Man2C1 KD2, or control vector. The expression level of *Man2C1* mRNA relative to *GAPDH* mRNA for each cell line was analyzed via quantitative real time PCR (*qPCR*). The relative expression level of *Man2C1* in control cells was set to 1. *B*, α-mannosidase activity assay in *Man2C1* knockdown cells. The cytosolic fraction of each cell line was extracted and subjected to an α-mannosidase assay. *C*, annexin V/PI staining analysis for *Man2C1* knockdown cells. HeLa parental cells, control cells (transfected with control empty vector) and two different types of *Man2C1* knockdown cells were harvested, stained with FITC-annexin V and PI, and subjected to flow cytometry analysis. The percentage values represent the population of annexin V^+/PI^- cells undergoing apoptosis. *D*, PI cell cycle analysis of *Man2C1* knockdown cells. The percentage values indicate the population of sub-G_1 cells, indicative of apoptotic cells. All data were obtained from three independent experiments; the *error bars* represent the ± S.D. *, $p < 0.05$; **, $p < 0.001$.

TABLE 1

Size fractionation HPLC measurements of free oligosaccharides in the cytosol of HeLa cells with modulated expression of wild-type or mutant Man2C1

Oligosaccharides	HeLa Control	Man2C1 KD1	Man2C1 KD2	Man2C1 KD1 + WT	Man2C1 KD2 + WT	Man2C1 KD1 + D372A	Man2C1 KD2 + D372A
				pmol/10^6 cells			
$Hex_5HexNAc$	3.6	0.72	0.73	4.8	4.3	0.84	0.89
$Hex_6HexNAc$	2.3	3.7	3.3	1.1	1.6	3.7	3.3
$Hex_7HexNAc$	1.9	4.4	4.4	0.68	0.71	4.9	4.0
$Hex_8HexNAc$	6.2	13	13	2.4	2.1	18	14
$Hex_9HexNAc$	6.1	12	12	1.1	1.0	15	11

activated caspase 3 (27). A drastic increase of processed PARP (~89 kDa) was evident in cells stably expressing either Man2C1 shRNA (Fig. 3*B*, *lanes 3* and *4*) and in cells transiently transfected with either Man2C1 shRNA (Fig. 3*C*, compare *lanes 2* and *3* with *lane 1*). Taken together, these results clearly indicated that Man2C1 suppression resulted in caspase 3 activation and in turn increased the occurrence of the cleaved form of PARP.

Having confirmed caspase 3 activation, we next studied several upstream apoptotic signals. First, processing of two initiator caspases (caspases 8 and 9) was examined. Several major signaling pathways induce apoptosis in mammalian cells (28–31). In the extrinsic pathway, a signaling pathway is initiated by binding between the death receptor and the apoptotic ligands; pro-caspase 8 is then recruited and activated to further activate caspase 3 (32, 33). In the intrinsic pathway, death signals stimulate translocation, oligomerization, and insertion of Bax and/or Bak into the outer mitochondrial membrane; this insertion causes the release of several proteins, including cytochrome *c*, from the mitochondria and leads to pro-caspase 9 activation and subsequent caspase 3 activation (34). Caspase-3 is ultimately activated in both pathways but via distinct initiator

caspases: caspase 8 for the extrinsic pathway and caspase 9 for the intrinsic pathway.

Pro-caspase 8 levels did not differ between control and *Man2C1* knockdown cells, nor did levels of cleaved (active) caspase 8 (Fig. 3*D*, *top panel*, *lanes 3* and *4*); these findings clearly indicated that the *Man2C1* knockdown-induced apoptotic signal did not occur via the death receptor-mediated extrinsic pathway. In sharp contrast, levels of the active form of caspase 9 (37 kDa/35 kDa) were higher in *Man2C1* knockdown cells than in control cells (Fig. 3*D*, *middle panel*, *lanes 3* and *4*), suggesting that *Man2C1* knockdown-induced apoptosis operated via the mitochondria-dependent intrinsic pathway.

To further confirm that mitochondria-mediated cell death occurred in *Man2C1* knockdown cells, mitochondrial cytochrome *c* release to cytosol was assessed in these cells because this phenomenon precedes activation of caspase 9-dependent apoptosis (35). The levels of cytosolic cytochrome *c* were higher in *Man2C1* knockdown cells than in control cells, and conversely, levels of mitochondrial cytochrome *c* were lower in knockdown cells than in control cells (Fig. 3*E*, *lanes 3* and *4*). Taken together, these results indicated that Man2C1 down-regulation stimulated release of mitochondrial cytochrome *c* to the cytosol and thereby induced the caspase 9-dependent apoptotic signaling pathway.

Man2C1 Down-regulation Causes Enhanced CHOP Expression without Triggering ER Stress—The intrinsic apoptotic pathway can be induced by accumulation of unfolded or misfolded proteins in the ER (36–38). CHOP, often used as a marker for activation of ER stress, is believed to be the key molecule mediating mitochondria-dependent apoptosis triggered by ER stress (36–39). Having shown that Man2C1 down-regulation caused mitochondria-dependent apoptosis, we next investigated whether CHOP was involved in this phenomenon. Surprisingly, shRNA-mediated Man2C1 down-regulation led to a drastic increase in CHOP expression in HeLa cells (Fig. 4*A*,

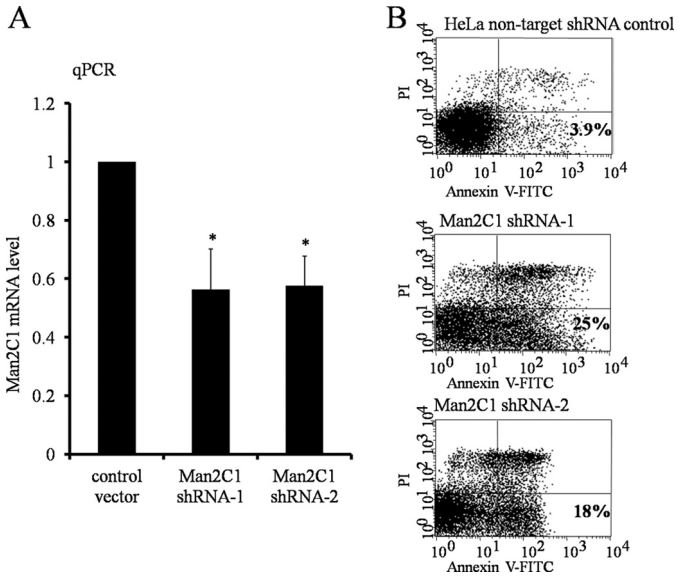

FIGURE 2. **Effect of transient transfection of HeLa cells with *Man2C1* shRNA.** *A*, quantitative real time PCR (*qPCR*) analysis of cells experiencing transient *Man2C1* knockdown. Relative expression level of *Man2C1* (normalized to *GAPDH* expression) in control cells was set to 1. The data represent the means ± S.D. from three independent experiments. *, $p < 0.05$. *B*, annexin V/PI staining analysis of cells experiencing transient *Man2C1* knockdown. MISSION nontarget shRNA control vector (SHC002; Sigma), which contains an shRNA insert that does not target any human or mouse gene, was used as the negative control shRNA. The data shown are results representative of three independent experiments.

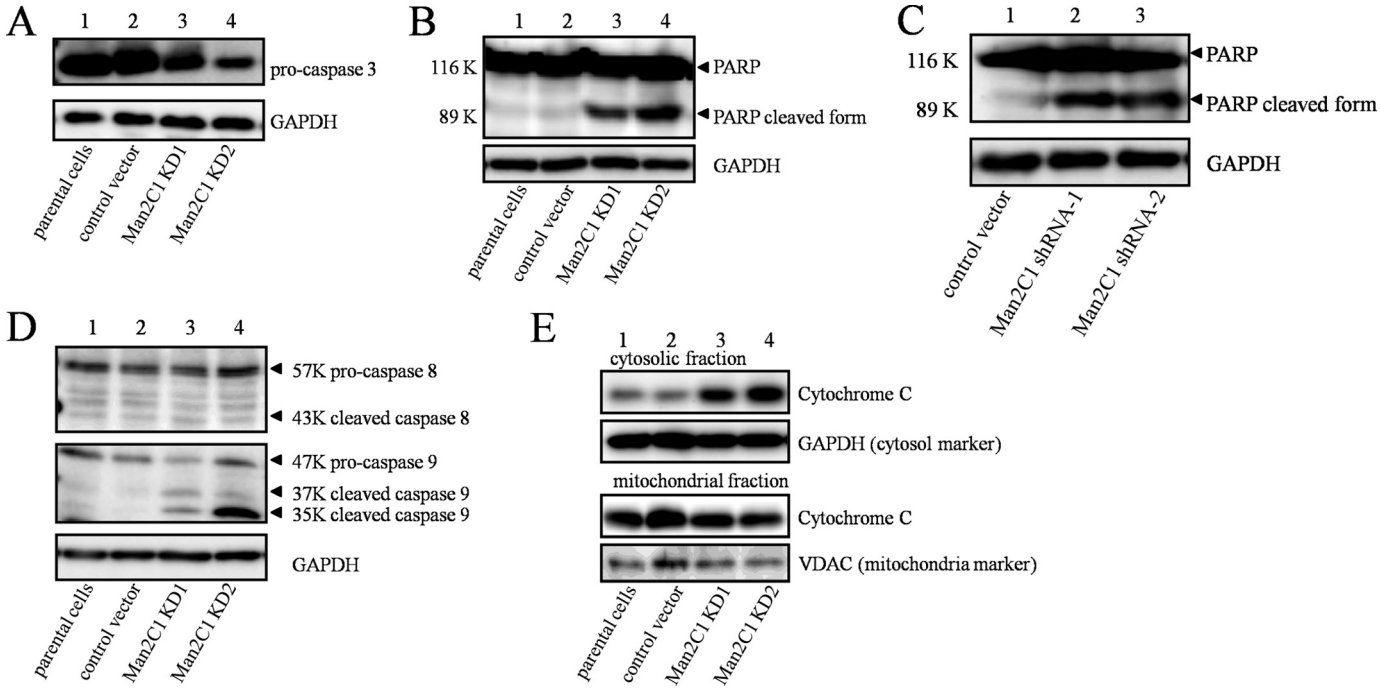

FIGURE 3. **Man2C1 down-regulation induced mitochondria-dependent apoptosis.** *A*, Western blot analysis of pro-caspase 3. *B*, Western blot analysis of PARP. The 116-kDa band represents the intact PARP, whereas the 89-kDa band represents the cleaved form of PARP, a hallmark of apoptotic signaling. *C*, Western blot analysis of PARP in cells transiently expressing control or Man2C1 shRNA. *D*, Western blot analysis of caspase 8 and caspase 9 (GAPDH; loading control (*A*–*D*)). *E*, subcellular fractionation of cytochrome *c* in Man2C1 knockdown cells. GAPDH and VDAC were as markers/loading controls for the cytosol and mitochondria fractions, respectively. The data shown are results representative of three independent experiments.

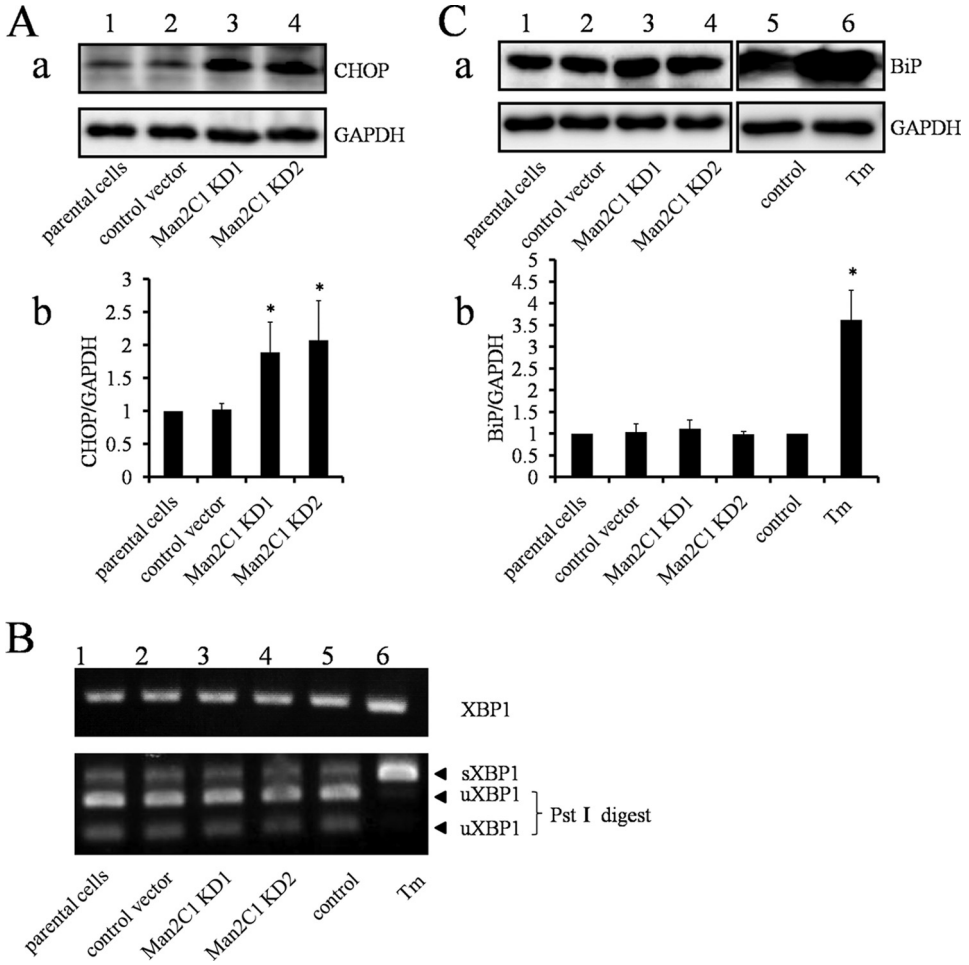

FIGURE 4. **CHOP expression was elevated in *Man2C1* knockdown cells without triggering ER stress.** *A*, analysis of CHOP protein in *Man2C1* knockdown cells. *Panel a*, Western blot analysis of CHOP in *Man2C1* knockdown cells. *GAPDH*, loading control. *Panel b*, measurement of the CHOP protein in *panel a*. *B*, *XBP1* splicing in *Man2C1* knockdown cells. To distinguish spliced *XBP1* (*sXBP1*) from unspliced *XBP1* (*uXBP1*), PstI digestion was carried out on PCR products. As a positive control representing the ER stress condition, cells were treated with 10 μM of tunicamycin (*Tm*) for 24 h (*lane 6*). *C*, analysis of BiP protein in *Man2C1* knockdown cells. *Panel a*, Western blot analysis of CHOP in *Man2C1* knockdown cells. *GAPDH*, loading control. *Panel b*, quantitation of the BiP protein in *panel a*. Tunicamycin-treated cells were used as a positive control for cells under ER stress (*lane 6*). The data represent the means from three independent experiments. The *error bars* represent the ± S.D. *: $p < 0.05$.

compare *lanes 3* and *4* with *lanes 1* and *2*), indicating that CHOP was involved in the apoptosis induced by Man2C1 down-regulation.

Although CHOP increased in *Man2C1* knockdown cells, ER stress signaling was not evident because *sXBP1* (the spliced form of the *XBP1* gene product and a marker for ER stress (37)) was not evident in these cells (Fig. 4*B*, *lanes 3* and *4*). Similarly, BiP, a major ER chaperone that is up-regulated upon ER stress, was not up-regulated in *Man2C1* knockdown cells (Fig. 4*C*, *lanes 3* and *4*). Taken together, these results indicated that ER stress may not be involved in the *Man2C1* knockdown-induced apoptosis and that up-regulation of CHOP could occur in an ER stress-independent fashion.

Down-regulation of Man2C1-induced Apoptosis Is Independent of the Man2C1 α-Mannosidase Activity—Man2C1 is the α-mannosidase involved in the catabolic pathway that processes free oligosaccharides in the cytosol (5, 7, 8, 15, 17, 40). We and others previously identified *in vivo* inhibitors of this enzyme (14, 16). Interestingly, although we saw increased free oligosaccharides in the cytosol, we did not observe any cell growth defect in the presence of this inhibitor (16). This result is in sharp contrast to the gene suppression-induced growth arrest/apoptosis observed in previous studies (12, 21), as well as in this study. Therefore, we hypothesized that the apoptosis induced by Man2C1 knockdown was not related to the enzymatic function of Man2C1.

To test this hypothesis, we introduced an enzymatically inactive form of *Man2C1*, in which Asp-372 was converted to Ala, into *Man2C1* knockdown cells to see whether this mutant rescued the apoptotic phenotype caused by the shRNA. The mutated aspartic acid residue is reportedly a catalytic residue that is conserved among family 38 α-mannosidases (41). After introduction of a wild-type or mutant *Man2C1* gene, mRNA levels of wild-type and mutant *Man2C1* increased significantly in the respective cells (Fig. 5*A*). This observation was consistent with the observations that cytosolic α-mannosidase activity increased in transfected cells expressing wild-type *Man2C1*, but not in cells expressing the catalytically inactive mutant Man2C1 (D372A) (Fig. 5*B*). Consistent with the cytosolic α-mannosidase activity, high mannose-type free oligosaccharides accumulated in *Man2C1* knockdown cells were processed by introduction of wild-type Man2C1, but not by introduction

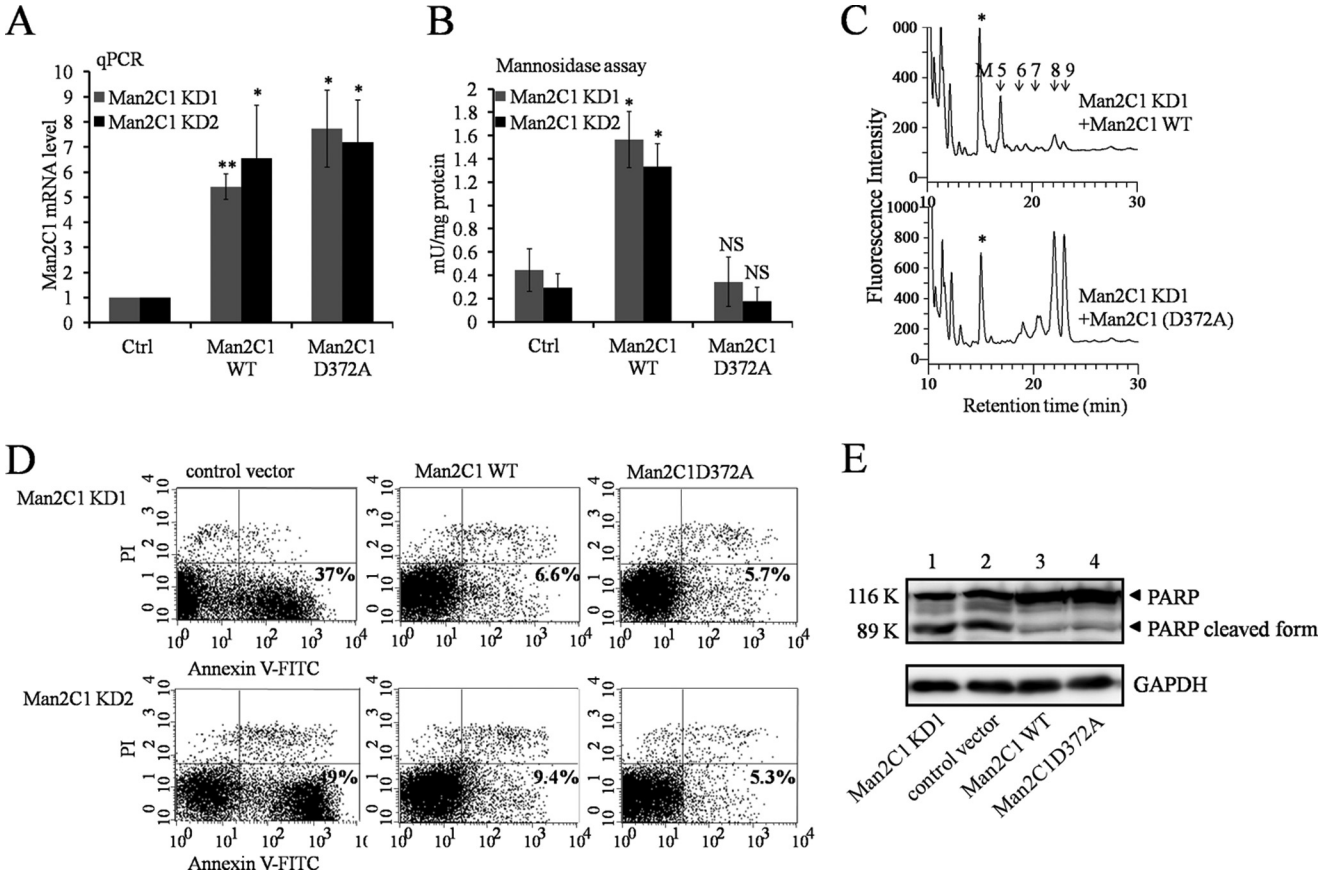

FIGURE 5. **Regulation of apoptosis by Man2C1 was independent of Man2C1 enzyme activity.** *A*, quantitative real time PCR (*qPCR*) analysis of both WT *Man2C1* and enzyme-dead mutant *Man2C1* (D372A) in transfected cells. *B*, α-mannosidase activity assay. *C*, profile of size fractionation HPLC for cytosolic, PA-labeled free oligosaccharides. *, α-mannosidase-insensitive, nonspecific peak. *M5–9* represent the elution positions for authentic $Man_{5-9}GlcNAc$ glycans obtained from RNase B. *D*, annexin V/PI staining analysis. The percentage values represent the population of annexin V^+/PI^- cells undergoing apoptosis. *E*, Western blot analysis of PARP/cleaved PARP. *GAPDH*, loading control; *Ctrl*, control. The *error bars* represent the ± S.D. from three independent experiments. *, $p < 0.05$; **, $p < 0.001$. *NS*, not significant.

of the catalytically inactive Man2C1 (D372A) mutant (Fig. 5*C* and Table 1). Interestingly, expression of either wild-type or mutant Man2C1 (D372A) clearly rescued the apoptotic phenotype in *Man2C1* knockdown cells, as shown by annexin V/PI staining (Fig. 5*D*). Moreover, immunoblot analysis indicated that PARP cleavage decreased in transfectants carrying either *Man2C1* transgene, irrespective of the presence or absence of the mannosidase-inactivating mutation (Fig. 5*E*, *lanes 3* and *4*). Taken together, these results clearly demonstrated that the regulatory function of Man2C1 in apoptosis was independent of the mannosidase activity.

Recently, He *et al.* (20) reported that full-length Man2C1 or N- or C-terminal truncations of Man2C1 attenuate phosphatase and tensin homolog (PTEN) functions by binding to PTEN. To determine whether truncated fragments of Man2C1 could rescue the apoptosis induced by Man2C1 shRNA, we constructed V5-tagged forms of full-length Man2C1 and of N- and C-terminally truncated Man2C1 (Fig. 6*A*). Each of the V5-tagged Man2CI fusion proteins were expressed in *Man2C1* knockdown cells (Fig. 6*B*); neither N-Man2C1 nor C-Man2C1 rescued apoptosis, as indicated by PARP cleavage (Fig. 6*C*, *lanes 3* and *4*); in sharp contrast, full-length Man2C1 suppressed the cleavage of PARP (Fig. 6*C*, *lane 2*).

Suppression of Man2C1 Also Results in Apoptosis in Other Cell Types—To further confirm that down-regulation of Man2C1 caused apoptosis in mammalian cells, we tested the effect of shRNA-mediated Man2C1 knockdown in two other types of human-derived cultured cells, MKN45 cells (gastric adenocarcinoma) and HepG2 cells (hepatocellular carcinoma). Each type of *Man2C1* shRNA was independently transiently transfected into each cell type. Transient transfection of either *Man2C1* shRNA caused decreased *Man2C1* expression in both cell types (Fig. 7, *A* and *C*), and in both cell types, increased PARP cleavage was observed (Fig. 7, *B* and *D*, *lanes 2* and *3*), clearly indicating that suppression of Man2C1-induced apoptosis was not specific to HeLa cells.

DISCUSSION

Man2C1 is a cytosolic α-mannosidase commonly found in vertebrates and is known to catabolize free oligosaccharides that have accumulated in the cytosol (12, 14–17). Overexpression and suppression of the *Man2C1* gene each reportedly have multiple phenotypic consequences. In one investigation, transgene expression of *Man2C1* promoted tumor progress in mice (18); later it was found that Man2C1 overexpression could attenuate PTEN function in prostate cancer cells (20). Con-

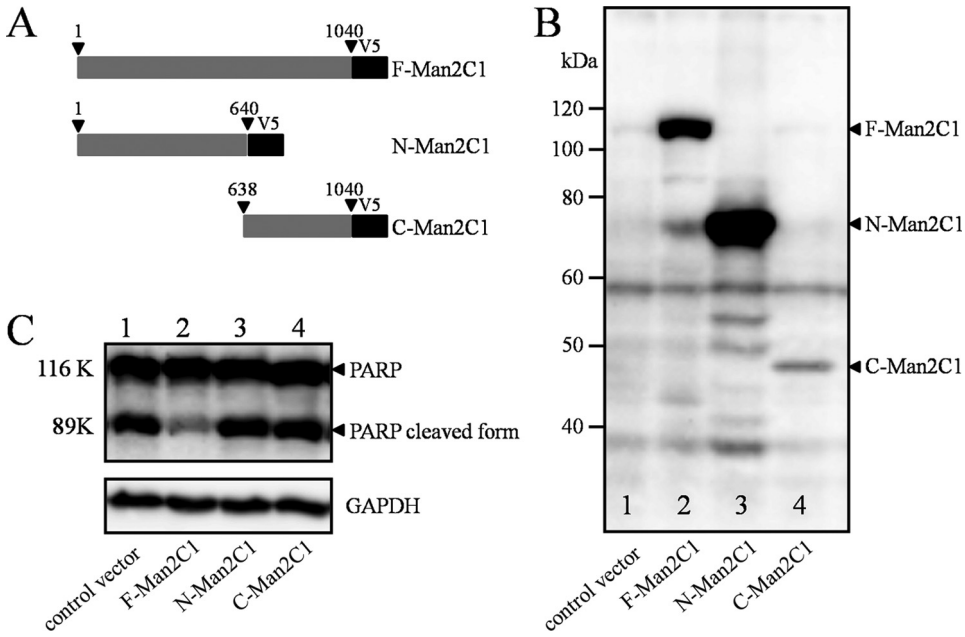

FIGURE 6. **Truncated fragments of Man2C1 cannot rescue the apoptosis induced by shRNA-mediated down-regulation of Man2C1.** *A*, schematic representation of each Man2C1 construct (full length (*F*); N-terminal fragment (*N*), and C-terminal fragment (*C*)). These proteins were tagged at their C-terminal end with V5 epitope for detection on Western blots. *B*, Western blot analysis of Man2C1 protein and Man2C1 truncation mutants. The *arrows* indicate the bands of intact proteins for each construct. *C*, Western blot analysis of PARP/cleaved PARP. *GAPDH*, loading control. The data shown are results representative of three independent experiments.

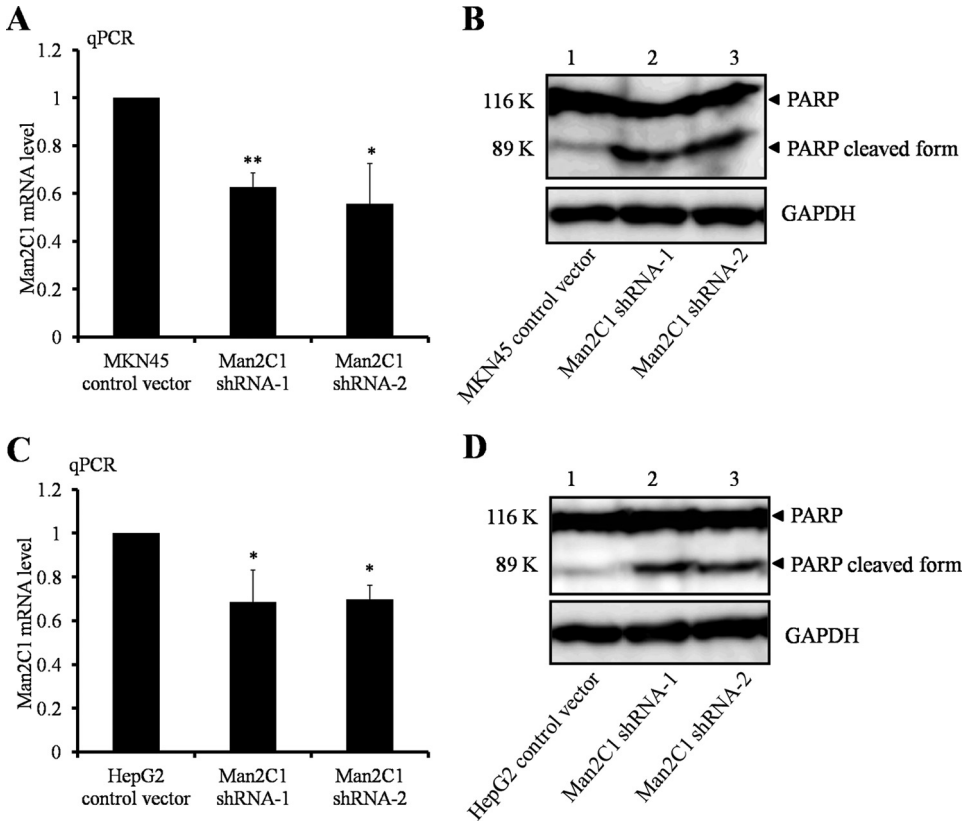

FIGURE 7. **Transient transfection of MKN45 cells or HepG2 cells with *Man2C1* shRNA.** *A* and *C*, quantitative real time PCR (*qPCR*) analysis of transiently transfected cells carrying *Man2C1* shRNA, MKN45 cells (*A*) and HepG2 cells (*C*). *B* and *D*, Western blot (*B*, MKN45 cells; *D*, HepG2 cells) analysis of PARP degradation. The *error bars* represent the ± S.D. from three independent experiments. *, $p < 0.05$; **, $p < 0.001$.

versely, suppression of Man2C1 expression could reduce the potentiality of tumor growth/metastasis (19, 21, 42). Most recently, methylation microarray analysis revealed that human subjects with higher levels of methylation at the *Man2C1* gene locus and greater exposure to post-traumatic events showed a marked increase in the risk of post-traumatic stress disorder

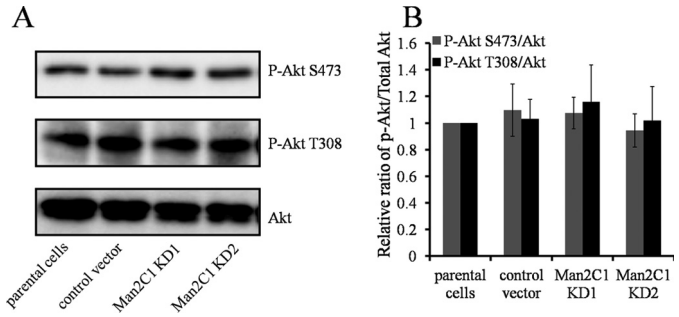

FIGURE 8. **Phosphorylation status of Akt was not altered because of suppression of Man2C1 expression.** *A*, Western blotting analysis for Akt/phosphorylated Akts in *Man2C1* knockdown HeLa cells. *B*, measurement of phosphorylated Akt (*P-Akt S473* or *P-Akt-T308*) in *A* as normalized to total Akt.

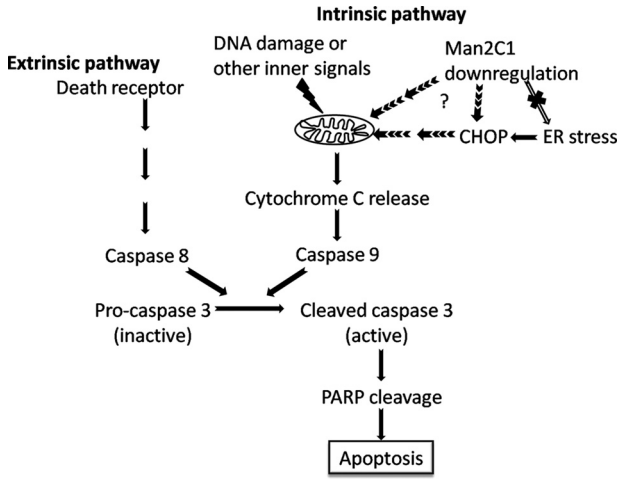

FIGURE 9. **Schematic representation of the extrinsic and intrinsic apoptosis signal pathways.** Man2C1 suppression seemed to activate the intrinsic pathway and act upstream of CHOP up-regulation, cytochrome *c* release from the mitochondria, caspase-9 activation, and caspase-3 activation.

relative to control subjects (43). None of these reports, however, successfully tied these phenotypic consequences with the Man2C1 enzymatic activity.

Bernon *et al.* (17) recently reported that Man2C1 overexpression could lead to increased intracellular mannose concentration and a consequent reduction in protein glycosylation, which in turn causes ER stress; these findings indicate that Man2C1 enzymatic activity does affect ER stress phenotypes. In contrast, we herein provide convincing evidence that Man2C1 also has an additional, enzyme-independent role as a key molecule regulating the intrinsic apoptosis signaling pathway.

Here, we demonstrated that suppression of Man2C1 caused HeLa cells to undergo mitochondria-dependent apoptosis through the up-regulation of CHOP. Interestingly, CHOP up-regulation did not depend on ER stress, because *Man2C1* knockdown—in sharp contrast to *Man2C1* overexpression (17)—did not elicit an unfolded protein response. CHOP is often used as a marker for ER stress activation, and it is a major player in ER stress-triggered apoptosis (36–38); nevertheless, the ER stress response can be induced independently of CHOP (44). Conversely, CHOP expression can be up-regulated independently of ER stress (45). Therefore, it appears possible that, following suppression of *Man2C1* expression, CHOP is somehow up-regulated independently of ER stress.

Most strikingly, the effect of Man2C1 on apoptosis was found to be independent of Man2C1 enzymatic activity, because a catalytically inactive form of Man2C1, like the wild-type protein, rescued the apoptotic phenotype in *Man2C1* knockdown cells. Our results indicated that Man2C1 had a nonenzymatic function in addition to its enzymatic function. Notably, orthologs of a cytoplasmic peptide:*N*-glycanase, which itself is involved in the catabolic pathway for free oligosaccharides, are reported to be catalytically inactive, although mutant forms of these orthologs exhibited severe phenotypes (46, 47). These observations led us to speculate that such enzyme-independent functions are not rare but are possibly an unrecognized feature of many cytosolic enzymes.

Man2C1 was recently identified as a PTEN-binding protein (20). He *et al.* (20) suggest that Man2C1, by binding to PTEN, attenuates PTEN functions; thus, Man2C1 up-regulation could promote tumorigenesis in prostate cancer cells. We did not observe any impaired PTEN signal, as judged by the level of phosphorylated Akt in two distinct lines of *Man2C1* knockdown cells (Fig. 8). Consistent with this result, we found that an N-terminal fragment of Man2C1 did not have anti-apoptotic activity; notably, this fragment was previously shown to be enough to inhibit the PIP3 phosphatase activity of PTEN (20). Currently, the role of PTEN, if any, in inducing apoptosis upon *Man2C1* knockdown remains unknown.

In summary, we have clearly shown that Man2C1 down-regulation induced apoptosis in HeLa cells via a mitochondria-dependent pathway. Notably, ER stress was not involved in CHOP up-regulation in the *Man2C1* knockdown cells (Fig. 9). This anti-apoptotic function of Man2C1 was shown to be independent of α-mannosidase activity; together, these findings provide convincing evidence that Man2C1 has a role in addition to that as a catabolic enzyme. Man2C1 up-regulation is reportedly involved in tumorigenesis of various cancer types; therefore, this protein has potential as an attractive target for anti-cancer therapy (16, 19). Further clarification of the mechanism by which Man2C1 down-regulation induces apoptosis will provide clues for designing Man2C1-based anti-cancer reagents in the future.

Acknowledgments—We thank the members of the Glycometabolome Team (RIKEN), particularly Drs. Yoichiro Harada and Yoshimi Haga, for helpful discussion and Sayako Iida for technical assistance. We also thank Dr. Takashi Angata (RIKEN) for valuable comments on this manuscript.

REFERENCES

1. Varki, A. (1993) Biological roles of oligosaccharides. All of the theories are correct. *Glycobiology* **3,** 97–130
2. Helenius, A., and Aebi, M. (2004) Roles of *N*-linked glycans in the endoplasmic reticulum. *Annu. Rev. Biochem.* **73,** 1019–1049
3. Haltiwanger, R. S., and Lowe, J. B. (2004) Role of glycosylation in development. *Annu. Rev. Biochem.* **73,** 491–537
4. Taniguchi, N., Miyoshi, E., Gu, J., Honke, K., and Matsumoto, A. (2006) Decoding sugar functions by identifying target glycoproteins. *Curr. Opin. Struct. Biol.* **16,** 561–566
5. Suzuki, T. (2007) Cytoplasmic peptide:*N*-glycanase and catabolic pathway for free *N*-glycans in the cytosol. *Semin. Cell Dev. Biol.* **18,** 762–769
6. Suzuki, T. (2009) Introduction to "Glycometabolome." *Trends Glycosci. Glycotechnol.* **21,** 219–227

7. Suzuki, T., and Funakoshi, Y. (2006) Free *N*-linked oligosaccharide chains. Formation and degradation. *Glycoconj. J.* **23,** 291–302
8. Chantret, I., and Moore, S. E. (2008) Free oligosaccharide regulation during mammalian protein *N*-glycosylation. *Glycobiology* **18,** 210–224
9. Vleugels, W., Duvet, S., Peanne, R., Mir, A. M., Cacan, R., Michalski, J. C., Matthijs, G., and Foulquier, F. (2011) Identification of phosphorylated oligosaccharides in cells of patients with a congenital disorders of glycosylation (CDG-I). *Biochimie* **93,** 823–833
10. Peric, D., Durrant-Arico, C., Delenda, C., Dupré, T., De Lonlay, P., de Baulny, H. O., Pelatan, C., Bader-Meunier, B., Danos, O., Chantret, I., and Moore, S. E. (2010) The compartmentalisation of phosphorylated free oligosaccharides in cells from a CDG Ig patient reveals a novel ER-to-cytosol translocation process. *PLoS One* **5,** e11675
11. Suzuki, T., Yano, K., Sugimoto, S., Kitajima, K., Lennarz, W. J., Inoue, S., Inoue, Y., and Emori, Y. (2002) Endo-β-*N*-acetylglucosaminidase, an enzyme involved in processing of free oligosaccharides in the cytosol. *Proc. Natl. Acad. Sci. U.S.A.* **99,** 9691–9696
12. Suzuki, T., Hara, I., Nakano, M., Shigeta, M., Nakagawa, T., Kondo, A., Funakoshi, Y., and Taniguchi, N. (2006) Man2C1, an α-mannosidase, is involved in the trimming of free oligosaccharides in the cytosol. *Biochem. J.* **400,** 33–41
13. Saint-Pol, A., Codogno, P., and Moore, S. E. (1999) Cytosol-to-lysosome transport of free polymannose-type oligosaccharides. Kinetic and specificity studies using rat liver lysosomes. *J. Biol. Chem.* **274,** 13547–13555
14. Butters, T. D., Alonzi, D. S., Kukushkin, N. V., Ren, Y., and Blériot, Y. (2009) Novel mannosidase inhibitors probe glycoprotein degradation pathways in cells. *Glycoconj. J.* **26,** 1109–1116
15. Chantret, I., Fasseu, M., Zaoui, K., Le Bizec, C., Yayé, H. S., Dupré, T., and Moore, S. E. (2010) Identification of roles for peptide. *N*-Glycanase and endo-β-*N*-acetylglucosaminidase (Engase1p) during protein *N*-glycosylation in human HepG2 cells. *PLoS One* **5,** e11734
16. Kato, A., Wang, L., Ishii, K., Seino, J., Asano, N., and Suzuki, T. (2011) Calystegine B3 as a specific inhibitor for cytoplasmic alpha-mannosidase, Man2C1. *J Biochem.* **149,** 415–422
17. Bernon, C., Carré, Y., Kuokkanen, E., Slomianny, M. C., Mir, A. M., Krzewinski, F., Cacan, R., Heikinheimo, P., Morelle, W., Michalski, J. C., Foulquier, F., and Duvet, S. (2011) Overexpression of Man2C1 leads to protein underglycosylation and upregulation of endoplasmic reticulum-associated degradation pathway. *Glycobiology* **21,** 363–375
18. Xiang, Z. G., Jiang, D. D., Liu, Y., Zhang, L. F., and Zhu, L. P. (2010) hMan2c1 transgene promotes tumor progress in mice. *Transgenic Res.* **19,** 67–75
19. Yue, W., Jin, Y. L., Shi, G. X., Liu, Y., Gao, Y., Zhao, F. T., and Zhu, L. P. (2004) Suppression of 6A8 α-mannosidase gene expression reduced the potentiality of growth and metastasis of human nasopharyngeal carcinoma. *Int. J. Cancer* **108,** 189–195
20. He, L., Fan, C., Kapoor, A., Ingram, A. J., Rybak, A. P., Austin, R. C., Dickhout, J., Cutz, J. C., Scholey, J., and Tang, D. (2011) α-Mannosidase 2C1 attenuates PTEN function in prostate cancer cells. *Nat. Commun.* **2,** 307
21. Tian, Y., Ju, J. Y., Zhou, Y. Q., Liu, Y., and Zhu, L. P. (2008) Inhibition of α-mannosidase Man2c1 gene expression suppresses growth of esophageal carcinoma cells through mitotic arrest and apoptosis. *Cancer Sci.* **99,** 2428–2434
22. Peña, J., and Harris, E. (2011) Dengue virus modulates the unfolded protein response in a time-dependent manner. *J. Biol. Chem.* **286,** 14226–14236
23. Hirayama, H., Seino, J., Kitajima, T., Jigami, Y., and Suzuki, T. (2010) Free oligosaccharides to monitor glycoprotein endoplasmic reticulum-associated degradation in Saccharomyces cerevisiae. *J. Biol. Chem.* **285,** 12390–12404
24. Tang, Q., Guo, K., Kang, K., Zhang, Y., He, L., and Wang, J. (2011) Classical swine fever virus NS2 protein promotes interleukin-8 expression and inhibits MG132-induced apoptosis. *Virus Genes* **42,** 355–362
25. Han, Y. H., Moon, H. J., You, B. R., Yang, Y. M., Kim, S. Z., Kim, S. H., and Park, W. H. (2010) MG132, a proteasome inhibitor, induced death of calf pulmonary artery endothelial cells via caspase-dependent apoptosis and GSH depletion. *Anticancer Res.* **30,** 879–885
26. Huang, T., Zhu, Y., Fang, X., Chi, Y., Kitamura, M., and Yao, J. (2010) Gap junctions sensitize cancer cells to proteasome inhibitor MG132-induced apoptosis. *Cancer Sci.* **101,** 713–721
27. Heeres, J. T., and Hergenrother, P. J. (2007) Poly(ADP-ribose) makes a date with death. *Curr. Opin. Chem. Biol.* **11,** 644–653
28. Igney, F. H., and Krammer, P. H. (2002) Death and anti-death. Tumour resistance to apoptosis. *Nat. Rev. Cancer* **2,** 277–288
29. Benedict, C. A., Norris, P. S., and Ware, C. F. (2002) To kill or be killed. Viral evasion of apoptosis. *Nat. Immunol.* **3,** 1013–1018
30. Boatright, K. M., and Salvesen, G. S. (2003) Mechanisms of caspase activation. *Curr. Opin. Cell Biol.* **15,** 725–731
31. Green, D. R. (2005) Apoptotic pathways. Ten minutes to dead. *Cell* **121,** 671–674
32. Sartorius, U., Schmitz, I., and Krammer, P. H. (2001) Molecular mechanisms of death-receptor-mediated apoptosis. *Chembiochem.* **2,** 20–29
33. Rath, P. C., and Aggarwal, B. B. (1999) TNF-induced signaling in apoptosis. *J. Clin. Immunol.* **19,** 350–364
34. Hagberg, H., Mallard, C., Rousset, C. I., and Xiaoyang, W. (2009) Apoptotic mechanisms in the immature brain. Involvement of mitochondria. *J. Child Neurol.* **24,** 1141–1146
35. Green, D. R., and Reed, J. C. (1998) Mitochondria and apoptosis. *Science* **281,** 1309–1312
36. Tabas, I., and Ron, D. (2011) Integrating the mechanisms of apoptosis induced by endoplasmic reticulum stress. *Nat. Cell Biol.* **13,** 184–190
37. Kim, I., Xu, W., and Reed, J. C. (2008) Cell death and endoplasmic reticulum stress. Disease relevance and therapeutic opportunities. *Nat. Rev. Drug Discov.* **7,** 1013–1030
38. Szegezdi, E., Logue, S. E., Gorman, A. M., and Samali, A. (2006) Mediators of endoplasmic reticulum stress-induced apoptosis. *EMBO Rep.* **7,** 880–885
39. Oyadomari, S., and Mori, M. (2004) Roles of CHOP/GADD153 in endoplasmic reticulum stress. *Cell Death Differ.* **11,** 381–389
40. Funakoshi, Y., and Suzuki, T. (2009) Glycobiology in the cytosol. The bitter side of a sweet world. *Biochim. Biophys. Acta* **1790,** 81–94
41. Howard, S., He, S., and Withers, S. G. (1998) Identification of the active site nucleophile in jack bean α-mannosidase using 5-fluoro-β-L-gulosyl fluoride. *J. Biol. Chem.* **273,** 2067–2072
42. Qu, L., Ju, J. Y., Chen, S. L., Shi, Y., Xiang, Z. G., Zhou, Y. Q., Tian, Y., Liu, Y., and Zhu, L. P. (2006) Inhibition of the α-mannosidase Man2c1 gene expression enhances adhesion of Jurkat cells. *Cell Res.* **16,** 622–631
43. Uddin, M., Galea, S., Chang, S. C., Aiello, A. E., Wildman, D. E., de los Santos, R., and Koenen, K. C. (2011) Gene expression and methylation signatures of MAN2C1 are associated with PTSD. *Dis. Markers* **30,** 111–121
44. Skalet, A. H., Isler, J. A., King, L. B., Harding, H. P., Ron, D., and Monroe, J. G. (2005) Rapid B cell receptor-induced unfolded protein response in nonsecretory B cells correlates with pro- versus antiapoptotic cell fate. *J. Biol. Chem.* **280,** 39762–39771
45. Lozon, T. I., Eastman, A. J., Matute-Bello, G., Chen, P., Hallstrand, T. S., and Altemeier, W. A. (2011) PKR-dependent CHOP induction limits hyperoxia-induced lung injury. *Am. J. Physiol. Lung Cell Mol. Physiol.* **300,** L422–L429
46. Maerz, S., Funakoshi, Y., Negishi, Y., Suzuki, T., and Seiler, S. (2010) The Neurospora peptide:*N*-glycanase ortholog PNG1 is essential for cell polarity despite its lack of enzymatic activity. *J. Biol. Chem.* **285,** 2326–2332
47. Funakoshi, Y., Negishi, Y., Gergen, J. P., Seino, J., Ishii, K., Lennarz, W. J., Matsuo, I., Ito, Y., Taniguchi, N., and Suzuki, T. (2010) Evidence for an essential deglycosylation-independent activity of PNGase in *Drosophila melanogaster*. *PLoS One* **5,** e10545